

Generation of stretched pulses and dissipative solitons at 2 μm from an all-fiber mode-locked laser using carbon nanotube saturable absorbers

YU WANG,^{1,*} SHAI-UL ALAM,² ELENA D. OBRAZTSOVA,³ ANATOLY S. POZHAROV,³ SZE Y. SET,¹ AND SHINJI YAMASHITA¹

¹ The University of Tokyo, Research Center for Advanced Science and Technology, 4-6-1 Komaba, Meguro-ku, Tokyo 153-8904, Japan

² Optoelectronics Research Centre, University of Southampton, Southampton SO17 1BJ, United Kingdom

³ A.M. Prokhorov General Physics Institute, RAS, 38 Vavilov Street, 11911, Moscow, Russia

*Corresponding author: wangyuhit13@cntp.t.u-tokyo.ac.jp

Received XX Month XXXX; revised XX Month, XXXX; accepted XX Month XXXX; posted XX Month XXXX (Doc. ID XXXXX); published XX Month XXXX

We demonstrate, for the first time to the best of our knowledge, a Thulium-doped all-fiber mode-locked laser using a carbon nanotube saturable absorber, operating in the dissipative-soliton regime and the stretched-pulse-soliton regime. The net dispersion of the laser cavity is adjusted by inserting different lengths of normal dispersion fiber, resulting in different mode-locking regimes. These results could serve as a foundation for the optimization of mode-locked fiber laser cavity design at the 2 μm wavelength region.

OCIS codes: (140.4050) Mode-locked lasers; (140.3510) Lasers, fiber; (140.3500)

<http://dx.doi.org/10.1364/OL.99.099999>

Mode-locked fiber lasers in the 2 μm spectral region are required in many applications – such as, free-space optical communications, atmospheric sensing, laser imaging detection and ranging (LIDAR). They are also indispensable compact pump sources for optical parametric oscillators to generate longer mid-infrared wavelengths via nonlinear conversion [1, 2]. Favorable absorption in water and some plastic materials at this wavelength range makes such lasers very useful for surgical applications and material processing [3]. Furthermore, 2 μm lasers are particularly attractive light sources for gas sensing, such as CO₂ detection [4].

As silica fibers generally exhibit a large anomalous dispersion at 2 μm , most of the reported mode-locked fiber lasers at this wavelength are operating in the soliton pulse regime [5]. Since soliton pulse requires a perfect balance between fiber dispersion and nonlinearity, the resulting pulse energy is usually restricted by the cavity design and the fiber type used.

Dispersion management has the potential to overcome this limitation. By adjusting the net dispersion to near zero, stretched-pulse solitons can be generated, which have the advantages of having a low

noise, a relatively high pulse energy, and a short pulse duration [6]. In addition, if the net dispersion becomes normal and relatively large, dissipative solitons can be generated. Although dissipative soliton pulse can possess a large energy, it proves difficult to compress such pulse perfectly outside the cavity, due to the large nonlinear effects associated with the evolution of the dissipative soliton [7, 8]. Theoretical study of pulse-shaping mechanisms of stretched pulses and dissipative solitons in Tm-doped fiber lasers have been done [9]. At the wavelength of 2 μm , the shortest pulse duration of 45 fs is achieved from a stretched-pulse mode-locked laser; whereby a piece of ZBLAN (ZrF₄-BaF₂-LaF₃-AlF₃-NaF) fiber is used for dispersion compensation, while nonlinear polarization rotation (NPR) acts as a fast saturable absorber [10]. Pulse energy as high as 4.3 nJ has been demonstrated from a stretched-pulse mode-locked laser where a bulk grating pair is used for dispersion compensation [11, 12] and pulse characteristics of such lasers has been theoretically studied [13]. Dissipative solitons, as well as stretched pulses at 2 μm have also been reported in a linear cavity using a chirped fiber Bragg grating (CFBG) for providing normal dispersion, and a semiconductor saturable absorber mirror (SESAM) to assist mode-locking [14]. In this reference, the cavity dispersion is tuned between -0.32 ps² to 0.41 ps² by adjusting the length of passive fiber which exhibits anomalous dispersion. In addition, grating pairs and NPR are used to generate dissipative solitons with a considerably high pulse energy of 8 nJ [15]. However, both NPR and SESAMs suffer from environmental stability issues.

In contrast, carbon nanotube (CNT) saturable absorbers (SA) have the advantages of compactness, fiber compatibility, and being able to operate in transmission-, reflection- and bi-directional-modes [16]. A mesh of CNTs deposited on a silver-mirror has been used to achieve mode-locking at 1.05 μm , 1.56 μm and 1.99 μm [17]. A tunable Ho-doped soliton fiber laser mode-locked by CNT is realized by adjustment of a polarization controller and scanning the spot on a CNT reflector [18]. As for dispersion management, a piece of dispersion compensation fiber (DCF) can be inserted in the laser cavity to control the overall cavity dispersion. Soliton pulse and stretched pulse

operation has been demonstrated by changing a length of DCF in a Tm/Ho-doped fiber laser mode locked by NPR [19].

Here, we demonstrate for the first time, to the best of our knowledge, stretched-pulse soliton and dissipative soliton generations at 2 μm using a length of DCF for cavity dispersion management and a CNT-SA as a mode-locker.

A similar experiment has been reported at 1.55 μm for the generation of high power, ultra-short pulses [20]. However, a distinct difference in our laser configuration is that the absence of a spectral filter in our laser cavity. Since chirped pulses are generated in both the stretched-pulse and the dissipative-soliton regimes, different parts of the pulses contain different spectral components. A saturable absorber, which serves as a temporal filter to compress and reshape the pulses at each cavity round trip, can also function as a spectral filter for the stabilization of laser mode locking. Elimination of the spectral filter allows us to reduce the cavity round trip loss, resulting in a decrease of mode locking threshold and an increase in output power. The schematic of the experimental setup is shown in Fig. 1. Carboxymethyl cellulose (CMC) is used as a host polymer for the carbon nanotubes because it has a flat absorption spectrum in the 1~2 μm wavelength region. The single-walled carbon nanotubes used were synthesized using the arc-discharge technique, which is the preferred technique to produce larger nanotube diameter for longer wavelength operation. The CMC is used as a surfactant for the dispersion of the CNT. The CNT is dispersed in the CMC solution via ultra-sonication with an initial CNT concentration of 2 % weight. The concentration of the CNT-CMC mixture is further condensed via ultracentrifugation, before the formation of the CNT polymer film by suspension drying. The resulting CNT polymer film has a strong absorption around 1960 nm as shown in Fig. 2. The film is sandwiched between two FC-UPC optical fiber connectors to serve as the SA device for laser mode locking.

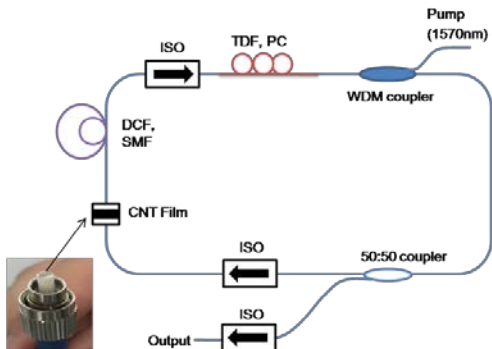


Fig. 1. Schematic of the ring-cavity Tm-doped fiber laser mode locked with a CNT-SA.

A 4m-long thulium-doped silica fiber (TDF) (OFS, TmDF200) is used as the gain media with an estimated anomalous dispersion of $-0.02 \text{ ps}^2/\text{m}$ at 1960 nm. The TDF is pumped through a wavelength-division multiplexing (WDM) coupler in a counter-directional pumping scheme. The pump source is an external-cavity tunable laser (Photonics, Tunics-Plus) operating at 1570 nm amplified by a high power Erbium-doped optical fiber amplifier (Keopsys, KPS-BT2-C-37). A fiber-loop-type polarization controller (PC) is inserted in the cavity for the study of the cavity polarization sensitivity. In order to reduce the length and the overall anomalous dispersion of the laser cavity, the TDF is used as the looping fiber in the PC. An isolator (ISO) is used to ensure unidirectional operation. A 50:50 coupler is used as the output coupler. A length of DCF (Sumitomo Electric, P-DCF) with an estimated normal dispersion of $0.07 \text{ ps}^2/\text{m}$ and a length of additional single-mode fiber (SMF) (Corning, SMF-28) with an estimated anomalous dispersion of $-0.06 \text{ ps}^2/\text{m}$ at 1960 nm are inserted between the ISO and the CNT saturable absorber for dispersion management. The pigtailed of all the

passive fiber components are made of SMF-28. The total cavity length without the DCF and the additional SMF for dispersion management is approximately 8 m. The mode-locking is self-starting once the pump power is increased above the threshold level without any adjustment of the PC. The threshold level is dependent on the length of the DCF and additional SMF inserted.

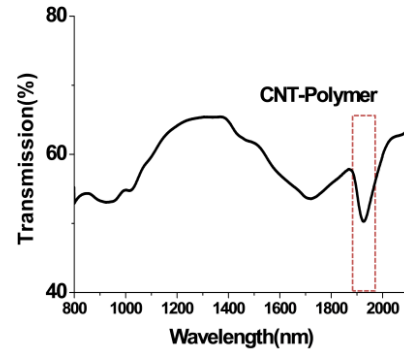


Fig. 2. Optical transmission spectrum of the CNT incorporated CMC film.

Fig. 3 shows the output spectra of the laser with different net dispersion settings. The spectrum is measured with an optical spectrum analyzer (ANDO, AQ6375) with an optical resolution bandwidth of 0.05 nm. When the net dispersion is -0.32 ps^2 , a typical soliton spectrum with Kelly sidebands is observed once the pump power is increased above the threshold level of 93 mW. The soliton spectrum has a 3 dB bandwidth of 4.0 nm. When we change the net dispersion to -0.02 ps^2 by inserting a 6 m-long DCF and a 1.8 m-long SMF, the spectral bandwidth increased to 7.5 nm. This spectral shape without Kelly sidebands is verified to be Gaussian shape, which indicates that the laser is in a stretched-pulse mode-locked regime. The threshold level of this stretched-pulse mode-locking is 115 mW.

The output spectral shape changes dramatically when the net dispersion of the laser cavity is set to 0.04 ps^2 by the insertion of a 6 m-long DCF and a 0.9 m-long SMF. Such spectrum with steep spectral edges is a clear signature of a dissipative-soliton operating regime. The threshold level in this operating regime is 125 mW. The output spectrum is broadened when the pump power is increased further, which is another signature of a dissipative-soliton operating regime. The 3 dB spectral bandwidth is measured to be 6.2 nm when the pump power is 130 mW. Unlike most of the previous works on dissipative solitons [20, 22], no spectral filter is used for the stabilization of mode-locking. The spectral filtering effect in our laser is initiated by the temporal filtering effect of the CNT-SA on a chirped pulse. The center wavelengths in the stretched-pulse regime and the dissipative-soliton regime are both blue-shifted compared to that of the soliton, due to the additional splice losses in the cavity between dissimilar fibers, the SMF and the DCF.

We measured the autocorrelation traces using a background free, second-harmonic generation (SHG) autocorrelator (Femtochrome, FR-103HP). Fig. 4 shows the autocorrelation trace of the soliton pulse when the net dispersion is set at -0.32 ps^2 . The autocorrelation width (T_{auto}) is measured to be 1.5 ps, inferring a full-width at half-maximum (FWHM) pulse width (T_{FWHM}) of 1.0 ps, assuming a hyperbolic-secant pulse shape. The time-bandwidth product (TBP) is 0.31 implying that the output pulse is a transform-limited soliton. Single-pulse operation is confirmed by a photodetector with 10GHz bandwidth (EOT, ET-5000) connected to a sampling oscilloscope (Agilent, DSO1024A). The fundamental repetition rate is 22.1 MHz, with a radio-frequency (RF) signal-to-noise ratio (SNR) of 60 dB, measured using an RF spectrum

analyzer (Agilent, E4440A) with 100 kHz span and 100Hz resolution bandwidth. The maximum pulse energy achieved under the single-pulse operation is 0.42 nJ.

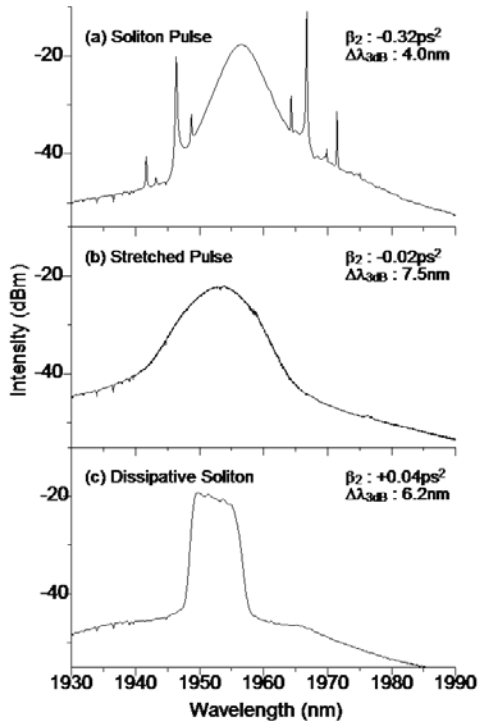


Fig. 3. Output spectra when the net dispersion is set at: (a) -0.32 ps^2 , (b) -0.02 ps^2 , and (c) 0.04 ps^2 , respectively.

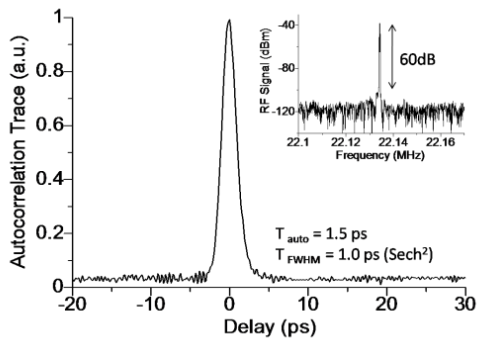


Fig. 4. The SHG autocorrelation trace of the soliton pulse when the net dispersion is set at -0.32 ps^2 . (Inset: the RF spectrum)

When the net dispersion is set at -0.02 ps^2 , the laser operates in the stretched-pulse regime. Fig. 6 shows the autocorrelation trace with an autocorrelation width of 3.8 ps, inferring a FWHM pulse width of 2.7 ps (assuming a Gaussian pulse shape). The TBP is 1.6 compared to the transform-limited value of 0.44, indicating that the pulses are chirped. The chirped output pulse is compressed externally using a length of SMF-28, as shown in Fig. 5. Due to the high loss in the pulse compressing fiber and the relatively low measurement sensitivity of the autocorrelator at this wavelength, an in-house built Tm-doped fiber amplifier is used to amplify the chirped pulses before launching into the pulse compressing fiber. The autocorrelation width of the dechirped pulse is 1.2 ps, with an inferred FWHM pulse width of 0.85

ps (Fig. 6). The TBP is estimated to be 0.49, which is close to the transform-limited value for Gaussian pulses of 0.44. Appearance of the small pedestals in the autocorrelation trace is attributed to the higher-order dispersion and the nonlinear effect associated with the amplification process. The fundamental repetition rate in this case is 11.7 MHz, with an RF-SNR of 55 dB. The maximum output pulse energy achieved before amplification in the stretched-pulse regime is 0.62 nJ, which is nearly 50 % higher than that in the soliton regime.

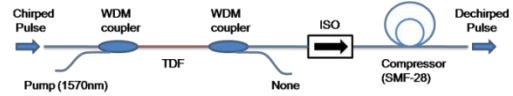


Fig. 5. Schematic of the pulse amplifier and compressor.

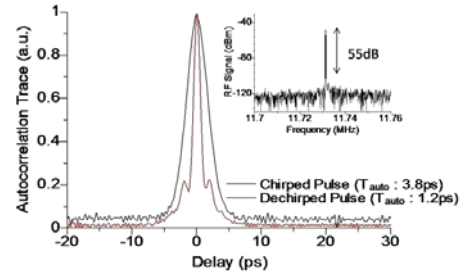


Fig. 6. Autocorrelation traces of the stretched pulse and the dechirped stretched pulse, with a cavity net dispersion set at -0.02 ps^2 . (Inset: the RF spectrum)

When the net dispersion is set at 0.04 ps^2 , the laser operates in the dissipative-soliton regime. The output pulse becomes highly chirped, with a measured autocorrelation width of 10.2 ps, and an inferred FWHM pulse width of 7.2 ps (assuming Gaussian pulse shape). The TBP of this highly-chirped dissipative soliton is estimated to be 4.9. The pulse is then compressed down to 0.95 ps (inferred from an autocorrelation width of 1.32 ps, Fig. 7), using a longer length of SMF-28.

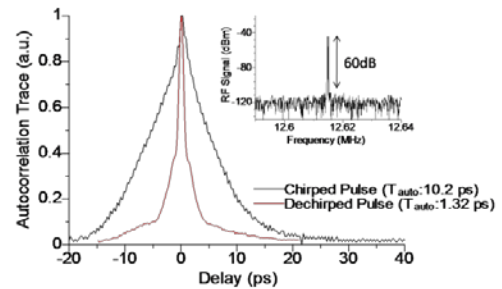


Fig. 7. Autocorrelation traces of the dissipative soliton and the dechirped dissipative soliton, when the net dispersion is set at 0.04 ps^2 . (Inset: the RF spectrum)

The TBP of the compressed pulse is 0.64, which is between the transform-limited value for a Gaussian pulse (0.44) and that of a pulse with a rectangular-spectrum (0.88). The triangular shape of the autocorrelation trace has been observed in phenomenon referred as dissipative soliton resonances [22]. A highly-chirped "temporal rectangular" pulse gives a triangular autocorrelation trace. The higher-order dispersion and the fiber nonlinear effect associated with the amplification process contribute to the minor deviation from the transform-limited pulse. The fundamental repetition rate is measured to be 12.6 MHz, with an RF-SNR of 60 dB. The maximum pulse energy

before amplification for the dissipative soliton is 0.70 nJ, similar to that of the stretched-pulse. A summary of the experimental parameters and results are shown in Table 1.

Table 1. Summary of the experimental parameters and results:

Operating Regime Parameter	Soliton Pulse	Stretched Pulse	Dissipative Soliton
Net Dispersion	-0.32 ps ²	-0.02 ps ²	0.04 ps ²
Additional Fiber	-	6 m DCF+2 m SMF	6 m DCF+1 m SMF
3dB Spectral Bandwidth	4.0 nm	7.5 nm	6.2 nm
T _{FWHM}	1.0 ps	2.7 ps	7.2 ps
Compressed T _{FWHM}	-	0.85 ps	0.95 ps
Max Pulse Energy	0.42 nJ	0.62 nJ	0.70 nJ
Threshold Pump Power	93 mW	115 mW	125 mW
RF Side Mode	60 dB	55 dB	60 dB

In conclusion, we have demonstrated that, by managing the cavity dispersion using a simple combination of appropriate fiber type and length, it is possible to achieve different mode-locking regimes.

We have also demonstrated for the first time, to the best of our knowledge, stretched pulse and the dissipative soliton generations through cavity dispersion management using a length of DCF and a CNT-SA for mode-locking, in the 2 μ m wavelength region. The CNT-SA also functions as a spectral filter for the stabilization of our laser. Unlike experimental lasers using NPR, CNT-SA allows key features such as self-starting, upgradability to an environmentally-stable all-polarization-maintaining-fiber version for robust industrial applications. Furthermore, the mode-locked laser, the pulse amplifier, and the compressor demonstrated here are in an all-fiber configuration with a potential for further high power scaling.

The generation of highly-chirped pulses in the dissipative-soliton regime can be extended to a chirped-pulse amplification system to achieve an extremely high peak power, which will be useful for various mid-infrared applications such as LIDAR and supercontinuum generations for gas sensing

Funding. Grants-in-Aid for Scientific Research (15H04012) of the Japan Society for the Promotion of Science (JSPS); “Femtosecond Optics and New Materials” program (RFBR-15-59-31817) of the Presidium of the Russian Academy of Sciences; Russian Science Foundation (RSF-14-22-00243)

Acknowledgment. We thank Sumitomo Electric Industries Ltd. and OFS for providing the dispersion properties of the DCF and the TDF, respectively. Dr. Shaif-ul Alam acknowledges the JSPS for awarding an Invitation Fellowship.

References

1. K. Scholle, S. Lamrini, P. Koopmann and P. Fuhrberg, in *Frontiers in Guided Wave Optics and Optoelectronics*, INTECH Open Access Publisher, 471 (2010)
2. P. A. Budni, L. A. Pomeranz, M. L. Lemons, C. A. Miller, J. R. Mosto, and E. P. Chicklis, *J. Opt. Soc. Am. B* **17**, 723 (2000).
3. J. Geng and S. Jiang, *Optics and Photonics News* **25**, 34 (2014)
4. B. Walsh, *Laser Phys.* **19**, 855 (2009).
5. M. A. Solodyankin, E. D. Obraztsova, A. S. Lobach, A. I. Chernov, A. V. Tausenev, V. I. Konov, and E. M. Dianov, *Opt. Lett.* **33**, 1336 (2008).

6. K. Tamura, E. P. Ippen, H. A. Haus, and L. E. Nelson, *Opt. Lett.* **18**, 1080 (1993).
7. A. Chong, W. H. Renninger, and F. W. Wise, *JOSA B* **25**, 140 (2008).
8. W. H. Renninger, A. Chong, and F. W. Wise, *JOSA B* **27**, 1978 (2010).
9. H. Li, J. Liu, Z. Cheng, J. Xu, F. Tan, and P. Wang, *Opt. Express* **23**, 6292 (2015).
10. Y. Nomura, and T. Fuji, *Opt. Express* **22**, 12461 (2014).
11. M. Engelbrecht, F. Haxsen, A. Ruehl, D. Wandt, and D. Kracht, *Opt. Lett.* **33**, 690 (2008).
12. F. Haxsen, A. Ruehl, M. Engelbrecht, D. Wandt, U. Morgner, and D. Kracht, *Opt. Express* **16**, 20471 (2008).
13. F. Haxsen, D. Wandt, U. Morgner, J. Neumann, and D. Kracht, *Opt. Express* **18**, 18981 (2010).
14. R. Gumenyuk, I. Vartiainen, H. Tuovinen, and O. G. Okhotnikov, *Opt. Lett.* **36**, 609 (2011).
15. Y. Tang, A. Chong, and F. W. Wise, *Opt. Lett.* **40**, 2361 (2015).
16. S. Yamashita, *J. Lightwave Technol.* **30**, 427 (2012).
17. S. Kivistö, T. Hakulinen, A. Kaskela, B. Aitchison, D. P. Brown, A. G. Nasibulin, E. I. Kauppinen, A. Härkönen, and O. G. Okhotnikov, *Opt. Express* **17**, 2358 (2009).
18. A. Yu. Chamorovskiy, A. V. Marakulin, A. S. Kurkov and O. G. Okhotnikov, *Laser Phys. Lett.* **9**, 602 (2012).
19. R. Kadel and B. R. Washburn, *Appl. Opt.* **54**, 746 (2015).
20. N. Nishizawa, Y. Nozaki, E. Itoga, H. Kataura, and Y. Sakakibara, *Opt. Express* **19**, 21874 (2011).
21. K. Kieu and F. W. Wise, *Opt. Express* **16**, 11453 (2008).
22. W. Chang, A. Ankiewicz, J. M. Soto-Crespo, and N. Akhmediev, *Phys. Rev. A* **78**, 23830 (2008).

Full References

1. K. Scholle, S. Lamrini, P. Koopmann and P. Fuhrberg, "2 μ m Laser Sources and Their Possible Application," in *Frontiers in Guided Wave Optics and Optoelectronics* (INTECH Open Access Publisher, 2010), p. 471.
2. P. A. Budni, L. A. Pomeranz, M. L. Lemons, C. A. Miller, J. R. Mosto, and E. P. Chicklis, "Efficient mid-infrared laser using 1.9- μ m-pumped Ho:YAG and ZnGeP2 optical parametric oscillators," *J. Opt. Soc. Am. B*, **17**, 723 (2000).
3. J. Geng, and S. Jiang, "Fiber Lasers: The 2 μ m Market Heats Up," *Opt. and Photon. News* **25**, 34 (2014).
4. B. Walsh, "Review of Tm and Ho materials; spectroscopy and lasers," *Laser Phys.* **19**, 855 (2009).
5. Max A. Solodyankin, E. D. Obraztsova, A. S. Lobach, A. I. Chernov, A. V. Tausenev, V. I. Konov, and E. M. Dianov, "Mode-locked 1.93 μ m thulium fiber laser with a carbon nanotube absorber," *Opt. Lett.* **33**, 1336 (2008).
6. K. Tamura, E. P. Ippen, H. A. Haus, and L. E. Nelson, "77-fs pulse generation from a stretched-pulse mode-locked all-fiber ring laser," *Opt. Lett.* **18**, 1080 (1993).
7. A. Chong, W. H. Renninger, and F. W. Wise, "Properties of normal-dispersion femtosecond fiber lasers," *JOSA B* **25**, 140 (2008).
8. W. H. Renninger, A. Chong, and F. W. Wise, "Area theorem and energy quantization for dissipative optical solitons." *JOSA B* **27**, 1978 (2010).
9. H. Li, J. Liu, Z. Cheng, J. Xu, F. Tan, and P. Wang, "Pulse-shaping mechanisms in passively mode-locked thulium-doped fiber lasers." *Opt. Express* **23**, 6292 (2015).
10. Y. Nomura, and T. Fuji, "Sub-50-fs pulse generation from thulium-doped ZBLAN fiber laser oscillator," *Opt. Express* **22**, 12461 (2014).
11. M. Engelbrecht, F. Haxsen, A. Ruehl, D. Wandt, and D. Kracht, "Ultrafast thulium-doped fiber-oscillator with pulse energy of 4.3 nJ," *Opt. Lett.* **33**, 690 (2008).
12. F. Haxsen, A. Ruehl, M. Engelbrecht, D. Wandt, U. Morgner, and D. Kracht, "Stretched-pulse operation of a thulium-doped fiber laser." *Opt. Express* **16**, 20471 (2008).
13. F. Haxsen, D. Wandt, U. Morgner, J. Neumann, and D. Kracht, "Pulse characteristics of a passively mode-locked thulium fiber laser with positive and negative cavity dispersion." *Opt. Express* **18**, 18981 (2010).
14. R. Gumenyuk, I. Vartiainen, H. Tuovinen, and O. G. Okhotnikov, "Dissipative dispersion-managed soliton 2 μ m thulium/holmium fiber laser," *Opt. Lett.* **36**, 609 (2011).
15. Y. Tang, A. Chong, and F. W. Wise, "Generation of 8 nJ pulses from a normal-dispersion thulium fiber laser," *Opt. Lett.* **40**, 2361 (2015).
16. S. Yamashita, "A tutorial on nonlinear photonic applications of carbon nanotube and graphene," *J. Lightwave Technol.* **30**, 427 (2012).
17. S. Kivistö, T. Hakulinen, A. Kaskela, B. Aitchison, D. P. Brown, A. G. Nasibulin, E. I. Kauppinen, A. Härkönen, and O. G. Okhotnikov, "Carbon nanotube films for ultrafast broadband technology," *Opt. Express* **17**, 2358 (2009).
18. A. Yu. Chamorovskiy, A. V. Marakulin, A. S. Kurkov and O. G. Okhotnikov, "Tunable Ho-doped soliton fiber laser mode-locked by carbon nanotube saturable absorber," *Laser Phys. Lett.* **9**, 602 (2012).
19. R. Kadel and B. R. Washburn, "Stretched-pulse and solitonic operation of an all-fiber thulium/holmium-doped fiber laser," *Appl. Opt.* **54**, 746 (2015).
20. N. Nishizawa, Y. Nozaki, E. Itoga, H. Kataura, and Y. Sakakibara, "Dispersion-managed, high-power, Er-doped ultrashort-pulse fiber laser using carbon-nanotube polyimide film," *Opt. Express* **19**, 21874 (2011).
21. K. Kieu, and F. W. Wise, "All-fiber normal-dispersion femtosecond laser," *Opt. Express* **16**, 11453 (2008).
22. W. Chang, A. Ankiewicz, J. M. Soto-Crespo, and N. Akhmediev, "Dissipative soliton resonances," *Phys. Rev. A* **78**, 23830 (2008).